Acoustic attenuation due to transformation twins in $CaCl_2$: analogue behaviour for stishovite

Zhiying Zhang[a,*], Wilfried Schranz[b], Michael A. Carpenter[a]

[a]Department of Earth Sciences, University of Cambridge, Downing Street, Cambridge CB2 3EQ, United Kingdom

[b]Faculty of Physics, University of Vienna, Strudlhofgasse 4, A-1090, Vienna, Austria

ABSTRACT

$CaCl_2$ undergoes a tetragonal ($P4_2/mnm$) to orthorhombic ($Pnnm$) transition as a function of temperature which is essentially the same as occurs in stishovite at high pressures. It can therefore be used as a convenient analogue material for experimental studies. In order to investigate variations in elastic properties associated with the transition and possible anelastic loss behaviour related to the mobility of ferroelastic twin walls in the orthorhombic phase, the transition in polycrystalline $CaCl_2$ has been examined using resonant ultrasound spectroscopy (RUS) at high frequencies (0.1-1.5 MHz) in the temperature interval 7-626 K, and dynamic mechanical analysis (DMA) at low frequencies (0.1-50 Hz) in the temperature interval 378-771 K. RUS data show steep softening of the shear modulus as the transition temperature is approached from above and substantial acoustic dissipation in the stability field of the orthorhombic structure. DMA data show softening of the storage modulus, which continues through to a minimum ~20 K below the transition point and is followed by stiffening with further lowering of temperature. There is no obvious acoustic dissipation associated with the transition, as measured by $\tan\delta$, however. The elastic softening and stiffening matches the pattern expected for a pseudoproper ferroelastic transition as predicted elsewhere. Acoustic loss behaviour at high frequencies fits with the pattern of behaviour expected for a twin wall loss mechanism but with relaxation times in the vicinity of ~10^{-6} s.

With such short relaxation times, the shear modulus of $CaCl_2$ at frequencies corresponding to seismic frequencies would include relaxations of the twin walls and is therefore likely to be significantly lower than the intrinsic shear modulus. If these characteristics apply also to twin wall mobility in stishovite, the seismic signature of the orthorhombic phase should be an unusually soft shear modulus but with no increase in attenuation.

Keywords: pseudoproper ferroelastic phase transition, ferroelastic twin walls, stishovite, $CaCl_2$, acoustic attenuation

1. Introduction

The high pressure phase transition in stishovite (SiO_2), between tetragonal ($P4_2/mnm$) and orthorhombic ($Pnnm$) structures, has attracted a great deal of recent attention both from its intrinsic interest in terms of physical properties related to pseudoproper ferroelastic behaviour (Tsuchida and Yagi 1989; Matsui and Tsuneyuki 1992; Cohen 1992, 1994; Lacks and Gordon 1993; Mao et al. 1994; Kingma et al. 1995, 1996; Lee and Gonze 1995, 1997; Dubrovinsky and Belonoshko 1996; Karki et al. 1997a,b; Andrault et al. 1998, 2003; Carpenter et al. 2000; Ono et al. 2002a; Carpenter 2006; Hemley et al. 1994, 2000a,b; Akins and Ahrens 2002; Shieh et al. 2002, 2005; Cordier et al. 2004; Tsuchiya et al. 2004; Lakshtanov et al. 2007b; Togo et al. 2008; Jiang et al. 2009; Bolfan-Casanova et al. 2009; Driver et al. 2010) and because these might have a direct influence on the seismic properties of subducted oceanic slabs (e.g. Kaneshima and Helffrich 2010; Vinnik et al. 2010; Nomura et al. 2010). From a geophysical perspective, the properties of interest are primarily elastic, and it is clear that the phase transition will give rise to marked softening of the shear modulus as the transition point is approached from the stability fields of both the tetragonal and orthorhombic structures as a consequence of softening of the single crystal elastic constants

($C_{11} - C_{12}$) (Cohen 1992, 1994; Matsui and Tsuneyuki 1992; Lacks and Gordon 1993; Lee and Gonze 1995; Dubrovinsky and Belonoshko 1996; Karki et al. 1997a, b; Hemley et al. 2000b; Carpenter et al. 2000; Shieh et al. 2002; Andrault et al. 2003; Carpenter 2006; Lakshtanov et al. 2007b; Togo et al. 2008; Jiang et al. 2009; Bolfan-Casanova et al. 2009; Driver et al. 2010). If the relevant mantle geotherm crosses the transition in PT space, it follows that the geophysical signal indicative of the presence of stishovite will be a characteristic pattern of velocity changes for both P and S waves. As in the case of the $\beta \leftrightarrow \alpha$ transition in quartz (e.g. Carpenter et al. 1998; Mechie et al. 2004; Carpenter 2006), knowledge of the phase boundary in PT space could then help to constrain the local geotherm. A much smaller anomaly is expected in the bulk modulus (e.g. Carpenter et al. 2000; Andrault et al. 2003; Carpenter 2006; Bolfan-Casanova et al. 2009), but this would be a more subtle effect and is altogether harder to detect even under laboratory conditions.

Another characteristic feature of ferroelastic phase transitions which is certainly relevant in the geophysical context is acoustic attenuation. This may be intrinsic in the vicinity of the transition point or extrinsic over a much wider interval of temperature and pressure due to the mobility under stress of twin walls in the low symmetry phase (e.g. Carpenter and Zhang 2011). Interest in anelastic effects more generally has been stimulated by the recognition that their temperature dependence is quite different from that of the elastic constants and, hence, that they could in principle provide a means of discriminating between the effects of temperature and composition (e.g. Romanowicz 1995; Karato and Karki 2001; Gung and Romanowicz 2004; Brodholt et al. 2007; Matas and Bukowinski 2007; Lekic et al. 2009; Carpenter and Zhang 2011). The expectation is that for most of the earth, seismic attenuation will be dominated by the anelastic properties of grain boundaries (e.g. Tan et al. 2001; Jackson et al. 2002; Webb and Jackson 2003; Faul and Jackson 2005; Jackson 2007; Salje 2008). However, recent investigations of the dynamics of twin walls in perovskites have

shown that loss mechanisms associated specifically with the mobility under dynamic stress of twin walls could be really quite substantial (e.g. Harrison and Redfern 2002; Harrison et al. 2004b, c; Carpenter et al. 2006; Daraktchiev et al. 2006, 2007; Walsh et al. 2008; McKnight et al. 2009a, b; Zhang et al. 2010a, b; Carpenter et al. 2010; Carpenter and Zhang 2011).

Such considerations immediately raise the question, as discussed in Carpenter et al. (2000), of whether there could also be significant attenuation of seismic waves due to the presence of transformation twins in orthorhombic stishovite and, if so, what temperature-, pressure- and frequency- dependence it might show. Unfortunately, these are not easy questions to address directly for stishovite itself due to the inherent difficulty in trying to measure anelastic properties at high pressures. An alternative and more tractable approach is to start with an analogue material which should show the same behaviour in principle but under more easily accessible laboratory conditions. The primary objective of the present study was to show unambiguously that twin-wall related loss mechanisms could occur in $CaCl_2$, which undergoes the same phase transition as occurs in stishovite but as a function of temperature at ambient pressure rather than as a function of pressure. Data are presented from resonant ultrasound spectroscopy (RUS) and dynamic mechanical analysis (DMA) at high frequencies (0.1-1.5 MHz) in the temperature interval ~7-626 K, and at low frequencies (0.1-50 Hz) in the temperature interval ~378-771 K, respectively.

As in stishovite, the $P4_2/mnm \leftrightarrow Pnnm$ transition in $CaCl_2$ is driven by a soft optic mode which induces softening of an acoustic mode by bilinear coupling of the order parameter with the symmetry-breaking strain (Unruh et al. 1992; Unruh 1993; Valgoma et al. 2002). From measurements of the lattice parameters and, hence, determinations of the spontaneous strain, it is known also that the transition is second order in both cases and is expected to conform closely to the precepts of Landau theory (Unruh 1993; Carpenter et al. 2000; Howard et al. 2005). The transition temperature, T_c, is ~491 K (Table 1; Bärnighausen

et al. 1984; Anselment 1985; Unruh et al. 1992; Unruh 1993; Howard et al. 2005). The same transition is also observed as a function of temperature in $CaBr_2$ (Raptis et al. 1989; Raptis and McGreevy 1991; Hahn and Unruh 1991; Unruh 1993; Kennedy and Howard 2004; Howard et al. 2005), and ferroelastic twins have been observed in this material by optical microscopy at room temperature (Unruh 1993). It is observed as a function of pressure in a much wider range of materials, including MgF_2 (Haines et al. 2001; Kanchana et al. 2003; Zhang et al. 2008; Kusaba and Kikegawa 2008b), FeF_2 (Wang et al. 2011), CoF_2 (Wang et al. 2011), NiF_2 (Wang et al. 2011), ZnF_2 (Perakis et al. 2005; Kusaba and Kikegawa 2008a), TiO_2 (Nagel and OKeeffe 1971; Fritz 1974), MnO_2 (Haines et al. 1995), GeO_2 (Haines et al. 1998, 2000; Lodziana et al. 2001; Ono et al. 2002b), RuO_2 (Haines and Leger 1993; Ono and Mibe 2011), SnO_2 (Haines and Leger 1997, 2003; Haines et al. 1997; Parlinski and Kawazoe 2000; Hellwig et al. 2003), PbO_2 (Haines et al. 1996), and MgH_2 (Zhang et al. 2007).

2. Experimental methods

Anhydrous $CaCl_2$ powder purchased from Sigma-Aldrich was ground using a mortar and pestle inside a glove box flushed with nitrogen gas. Pellets with diameter 13 mm were prepared by pressing the ground up powder under a pressure of 8 ton for 1 min. These were then fired in air using as follows: (1) heat from 373 K to 673 K at 5 K/min; (2) hold at 673 K for 2 h; (3) heat from 673 K to 773 K at 3 K/min; (4) hold at 773 K for 48 h; (5) cool from 773 K to 383 K at 3 K/min. Rectangular parallelepiped samples were cut from the pellets using an annular diamond saw lubricated with paraffin. For RUS measurements, the parallelepiped of $CaCl_2$ had dimensions $4.260 \times 3.143 \times 3.039$ mm^3, mass 0.0577 g. The density calculated from these dimensions is 1.418 g/cm^3, which is 64 % of the theoretical density, 2.20 g/cm^3, based on lattice parameters at 300 K given by Unruh (1993). Porosity leads to lower values of elastic moduli than in a fully dense sample (Ren et al. 2009). But the

interest here is in the pattern of changes through the phase transition rather than absolute values. For DMA tests, the sample had dimensions $1.268 \times 1.743 \times 3.713$ mm^3. Anhydrous $CaCl_2$ is very sensitive to moisture, and the samples were therefore kept in a desiccator with P_2O_5 powder as desiccant.

An offcut from the pellets used to make the RUS and DMA samples was crushed, immersed in a refractive index oil and examined in a polarizing optical microscope. Single birefringent grains up to ~5-10 μm wide could be seen and some of these contained planar or lamellar features, indicating the presence of transformation twins arising from the tetragonal → orthorhombic transition during cooling from the annealing temperature.

High temperature RUS data were collected in the frequency range 0.1-1.5 MHz with a step size of 28 Hz (50,000 data points per spectrum) using alumina buffer rods protruding into a horizontal Netzsch furnace (McKnight et al. 2008) and Stanford electronics described by Migliori and Maynard (2005). The sample was tested during repeated heating and cooling within the temperature range 386-626 K, with temperature steps of 2 K. During the last run, temperature was lowered to 291 K. The signal was generally weak but these repeated measurements revealed an overall pattern of peak variations which appeared to be systematic and which could be analyzed further. Low temperature RUS data were collected with the same frequency range and step sizes between 7 K and 307 K at 5 K intervals during cooling and heating using dynamic resonance system (DRS) Modulus II electronics and an Orange helium flow cryostat, as described by McKnight et al. (2007).

DMA measurements were undertaken by parallel plate compression using a Diamond DMA from PerkinElmer over the temperature range 378-771 K, with a heating and cooling rate of 3 K/min. Static (F_s) and dynamic forces (F_d) were applied in the frequency range 0.1-50 Hz using a steel rod. There is a phase lag, δ, between the applied force and the response of the sample, which is measured as the displacement of the rod, u_d. Energy dissipation is given

by

$$\tan\delta = E''/E', \quad (1)$$

where E'' is the loss modulus (i.e. the imaginary component of complex Young's modulus E) and E' is the storage modulus (i.e. real component of E) and the Young's modulus by

$$E = hF_{\mathrm{d}}\exp(\mathrm{i}\delta)/(Au_{\mathrm{d}}), \quad (2)$$

where h is the height of the sample, 3.713 mm, and A is the base area of the sample, 2.210 mm^2.

3. Results

Fig. 1 shows segments of RUS spectra in the form of stacks with offsets up the y-axis in proportion to the temperatures at which they were collected. Regularly spaced background peaks at high temperatures which do not change frequency to any great extent with temperature are due to the alumina buffer rods. At least some of the noisy background at very low temperatures arises from somewhere in the sample holder rather than from the sample itself. All the resonance peaks shift to lower frequency (elastic softening) with decreasing temperature and disappear below 481 K. They are not detectable in spectra collected in the high temperature instrument between 481 K and room temperature. Low amplitude peaks are easily visible in spectra from the low temperature instrument, however, due to the advantage of having the sample sitting directly on the transducers rather than at the end of alumina rods, remote from the transducers. With further decrease in temperature, the peaks shift to higher frequencies (elastic stiffening). At the lowest temperatures, weak peaks appear to be present but their trajectory is hard to follow due to noise.

The normalized square of frequency $(f/f_0)^2$ is proportional to the shear modulus,

$$(f/f_0)^2 = G/G_0 \quad (3)$$

assuming that the lowest frequency resonance peak depends exclusively on shearing. f_0 and G_0 are the resonance frequency and shear modulus at a reference temperature chosen here to be 626 K. Values of the inverse quality factor, Q^{-1}, were obtained from fitting an asymmetric Lorentzian function to individual resonance peaks as

$$Q^{-1} = \Delta f / f , \quad (4)$$

where f is the frequency of the peak and Δf its full width at half maximum amplitude. Strictly speaking, absolute values of Q^{-1} for comparison with other measures of damping should be obtained from fitting to the square of the amplitude, but the difference is only a factor of $\sim\sqrt{3}$ (see, for example, Lee et al. 2000; Lakes 2004). The resulting temperature dependences of G and Q^{-1} are shown in Fig. 2. Note that no data were obtained in the temperature range 306-481 K due to strong dissipation, or below ~105 K. Qualitative variations visible in the raw spectra (Fig. 1) are confirmed as being due to softening of the shear modulus as the expected tetragonal $\leftrightarrow$ orthorhombic transition temperature of 491 K (Bärnighausen et al. 1984; Anselment 1985; Unruh et al. 1992; Unruh 1993) is approached from either side. The total softening between 626 and 481 K is ~25 %. Values of Q^{-1} remain small (low attenuation) in the stability field of the tetragonal phase. Relatively high attenuation occurs throughout the temperature interval 105-306 K, over which peaks can be resolved in spectra from the orthorhombic phase.

The temperature dependences of E' and $\tan\delta$ obtained by DMA at frequencies of 0.1-50 Hz are shown in Fig. 3. Results for G and Q^{-1} obtained by RUS at ~0.3 MHz are also included for comparison. Note that the DMA data extend through the temperature interval between room temperature and 481 K where no RUS data were obtained. E' increases smoothly with falling temperature from 771 K to 651 K, essentially as would be expected for a material with normal thermal expansion, but then softening begins below ~550 K. There is a distinct, though rounded minimum at ~470 K which is not obviously dependent on frequency.

A smooth increase (stiffening) then occurs down to 378 K. This pattern of softening and stiffening below ~550 K is clearly associated with the expected phase transition. In marked contrast with the RUS results, however, there is no evidence for any acoustic loss as tanδ remains at a relatively low value for all frequencies at all temperatures below 650 K. Above ~650 K, there are significant increases in tanδ which vary systematically with frequency such that the steepest increase is seen at 0.1 Hz and the smallest increase at 50 Hz. These changes in tanδ at high temperatures also correlate, more or less, with changes in E', which shows mark softening at 0.1 Hz and nearly constant values at 50 Hz. A strong anelastic effect is implied and is most likely related to the influence of grain boundaries as the melting point (1045 K for anhydrous $CaCl_2$, Patnaik 2002) is approached.

4. Discussion

The $P4_2/mnm \leftrightarrow Pnnm$ transition in $CaCl_2$ displays all the classic features of a pseudoproper ferroelastic phase transition which is second order in character (Unruh et al. 1992; Unruh 1993, 1995; Valgoma et al. 2002). On the basis of lattice parameter data presented in Unruh (1993), the symmetry-breaking shear strain, $(e_1 - e_2)$, exceeds 4% at 0 K, and scales with temperature as $(e_1 - e_2) \propto Q^2 \propto (T_c^* - T)$, where Q is the order parameter and T_c^* is the transition temperature. In addition, there is a volume strain of over 1% which is made up of a large contraction in the (001) plane, $(e_1 + e_2) \approx -0.01$, and a much smaller contraction along [001], $e_3 \approx -0.001$. The transition is driven by a soft optic mode and the driving order parameter, Q, couples bilinearly with the symmetry-breaking strain as $\lambda(e_1 - e_2)Q$, where λ is a strain/order parameter coupling coefficient (Unruh et al. 1992; Unruh 1993). Based on Raman spectroscopic data for the soft mode and lattice parameter data to follow the strains, the overall pattern of behaviour is consistent with the expectations of

Landau theory (Unruh 1993). A more complete development of the Landau expansion to include predicted variations of the elastic constants has been presented elsewhere for the same transition as a function of pressure in stishovite (Carpenter et al. 2000, Hemley et al. 2000b, Carpenter 2006).

A quantitative description of the elastic properties of $CaCl_2$ would need data for the elastic constants of the tetragonal structure which are not yet available. Nevertheless, there are two particular observations which indicate how the bulk, shear and Young's moduli must vary qualitatively. Firstly, the strength of bilinear strain/order parameter coupling is indicated by the difference between T_c^* and the critical temperature, T_c, according to

$$T_c^* - T_c = \frac{\lambda^2}{a\frac{1}{2}\left(C_{11}^o - C_{12}^o\right)}, \quad (5)$$

where a is the coefficient of the Q^2 term in a normal Landau expansion and C_{11}^o and C_{12}^o are elastic constants of the tetragonal phase without influence from the transition. From Unruh et al. (1992) the value of $T_c^* - T_c$ is 247 K, consistent with the large observed shear strain and strong strain/order parameter coupling. This leads to a steep softening of $C_{11} - C_{12}$ as $T \rightarrow T_c^*$ from above and of $\overline{C}_{11} - \overline{C}_{12} = \frac{1}{2}\left(C_{11} + C_{22} - 2C_{12}\right)$ as $T \rightarrow T_c^*$ from below. The second directly relevant observation is the value of ~6.5 for the ratio of slopes of the square of the frequency of soft mode below and above T_c^* (Unruh et al. 1992). This ratio is also given by $2b/b^*$:1, where b is the coefficient of the fourth order term in the Landau coefficient and b^* its value as renormalized by coupling of the strains $\left(e_1 + e_2\right)$ and e_3 with Q^2. Such a large observed ratio implies a large renormalisation of b and this is consistent with the large observed values of $\left(e_1 + e_2\right)$ in Unruh (1993). Strong coupling of the order parameter with the non-symmetry breaking strains in this way leads to significant softening of the elastic constants $\overline{C}_{11} + \overline{C}_{12} = \frac{1}{2}\left(C_{11} + C_{22} + 2C_{12}\right)$, C_{33}, C_{13} and C_{23} of the orthorhombic structure. The

overall form of the expected elastic anomalies is therefore that given in Fig. 9 of Carpenter and Salje (1998) and reproduced here in Fig. 4. The bulk modulus will display the same pattern of evolution as shown for $\overline{C}_{11} + \overline{C}_{12}$, and the shear modulus will have a form which is a combination of $\overline{C}_{11} - \overline{C}_{12}$, C_{44}, C_{55} and C_{66}. The Young's modulus depends on both the shear modulus and the bulk modulus in the usual way ($E = 9KG/(3K+G)$). Thus the steep softening of G as $T \rightarrow T_c^*$ observed by RUS (Fig. 2) and the dip in E' through T_c^* observed by DMA (Fig. 3) are much as would be expected. This is entirely consistent with the pattern of elastic softening predicted for stishovite by Carpenter et al. (2000). Not included in the Landau description is the influence of fluctuations, which would give some additional softening as the transition is approached from above, particularly of the bulk modulus (cf. Carpenter and Salje 1998).

The primary objective of this study was to investigate the possibility of anelastic losses accompanying the ferroelastic transition in $CaCl_2$ as analogue behaviour for the extent to which SiO_2 with the stishovite structure might give rise to seismic attenuation in the Earth's mantle. At DMA frequencies, there is no evidence for any acoustic loss related to the transition and the question then arises as to whether this is due to the experimental conditions representing $\omega\tau >> 1$ or $\omega\tau << 1$. Here ω represents the angular frequency of the applied dynamical stress (= $2\pi f$ for f in Hertz) and τ the relaxation time of the twin walls; maximum dissipation occurs at $\omega\tau = 1$ according to the Debye equation (Nowick and Berry 1972). At RUS frequencies, the loss behaviour appears to be typical of the influence of ferroelastic twins, implying that the relaxation times for twin walls to respond to an external stress are in the vicinity of ~10^{-6} s and, hence, that DMA measurements represent the behaviour at $\omega\tau << 1$. Conventional transformation twins have been observed in single crystals of $CaBr_2$ (Unruh 1993) and, from the optical observations described above, it appears that twins were present in the polycrystalline sample used here.

Within the stability field of the tetragonal phase, Q^{-1} remains low in spite of the real issue of dealing with a difficult material to prepare and handle. It tends to increase when the transition temperature of 491 K (given by Bärnighausen et al. 1984; Anselment 1985; Unruh et al. 1992; Unruh 1993) is approached from above. Immediately below the transition temperature, the dissipation becomes sufficiently large that resonance peaks are not observed. This is characteristic of twin wall mediated superattenuation, as observed in $LaAlO_3$ (Carpenter et al. 2010). In the interval where there are no data, a plateau of attenuation would then be expected, by analogy with the dissipation behaviour of both acoustic and dielectric properties at ferroelectric transitions, which is attributed to viscous movement of twin walls. The viscous drag may be understood in terms to the disruption of phonons behind the moving walls (Combs and Yip 1983; Huang et al. 1992; Wang et al. 1996; Harrison et al. 2004a). At lower temperatures, the improved resolution of the low temperature RUS head reveals the presence of broad RUS peaks with a tendency for Q^{-1} to reduce with falling temperature, corresponding to the lower temperature part of the expected plateau region. Below ~100 K the peaks seem again to disappear though some relatively sharp resonances may be present in the rather noisy spectra collected at the lowest temperatures. A peak of dissipation in this temperature range would be due to freezing of the twin wall motion if it follows the characterstic behaviour of other systems. Hence, although the data for Q^{-1} are incomplete, the present observations are at least consistent with the pattern of loss behaviour reported for $LaAlO_3$ by Harrison et al. (2004c) (and see Fig. 6 of Carpenter et al. 2010). This pattern is shown by the dash-dotted curve in Fig. 2b.

From these observations it appears that $CaCl_2$ behaves in exactly the manner expected for other ferroelastic materials with respect to strain evolution, elastic softening and acoustic losses. There is no reason to suppose that the softening and dynamic loss mechanisms would be any different for essentially the same transition in stishovite and the only remaining

298 questions, in terms of analogue properties, are the relative magnitudes of strain/order
299 parameter coupling, for the softening, and the relative relaxation times of twin wall motion,
300 for the dissipation. The magnitudes of strain coupling effects are already reasonably well
301 constrained for stishovite (Carpenter et al. 2000; Hemley et al. 2000b) while relaxation times
302 will need to be determined experimentally. If the relaxation behaviour is more or less the
303 same between the two systems, it follows that the velocities of seismic waves through a rock
304 containing twinned, orthorhombic stishovite should be determined by the relaxed elastic
305 constants, i.e. including substantial motion of the twin walls. Comparison with experimental
306 results from single crystals of $LaAlO_3$ perovskite at low frequencies in its superelastic regime
307 (Harrison and Redfern 2002; Harrison et al. 2004b) suggest that the effective value of
308 $\overline{C}_{11} - \overline{C}_{12}$ could be as low as ~10% of the intrinsic value which excludes the influence the
309 twin walls. In a polycrystalline sample, i.e. a rock, the total magnitude of the twin wall related
310 softening will be less than this, because only some proportion of the grains will have twin
311 walls orientated in such a way that they experience the maximum displacement in response to
312 a given orientation of shear stress (Harrison et al. 2003). Even so, the effective softening
313 should still be greater than the intrinsic softening arising from strain/order parameter coupling
314 and the effective shear modulus will be similarly reduced. Harrison et al. (2003) also pointed
315 out that even a small degree of preferred orientation for twinned ferroelastic crystals could
316 lead to enhanced seismic anisotropy because of the sensitivity of twin wall motion to the
317 orientation of an applied shear stress.

318 In conclusion from the present considerations of $CaCl_2$, the geophysical signal for the
319 presence of orthorhombic stishovite in the mantle should be lowering of acoustic velocities
320 but without significant attenuation. Only if the relaxation times are substantially slower in
321 stishovite, due to the differences in bonding (particularly for rotations of adjacent octahedral
322 against each other in the (001) plane) or to pinning of the twin walls by impurities such as H

or Al, would the softening be accompanied by an increase in attenuation. There is still some uncertainty over the location of the phase transition in PT space (Ono et al. 2002a; Tsuchiya et al. 2004; Nomura et al. 2010) and of the effect of Al or H impurities (Lakshtanov et al. 2007a, b). It is therefore not yet clear exactly where stishovite in subducted oceanic crust would transform to the orthorhombic structure, but there are now at least clear patterns of predicted elastic and anelastic behaviour for comparison with geophysical observations.

Acknowledgements

Paul A. Taylor, Richard Thomson, Ming Zhang, Armin Fuith and Marius Reinecker kindly provided help with experiments. The RUS facilities in Cambridge were established through a grant from the Natural Environment Research Council (grant no. NE/B505738/1) and the present work was funded through grant no. NE/F017081/1. Support for the DMA facilities in Vienna was provided by the Austrian FWF (grant no. P19284-N20).

References

Akins, J.A., Ahrens, T.J., 2002. Dynamic compression of SiO_2: a new interpretation, Geophys. Res. Lett. 29, 1394.

Andrault, D., Angel, R.J., Mosenfelder, J.L., Le Bihan, T., 2003. Equation of state of stishovite to lower mantle pressure, Am. Mineral. 88, 301-307.

Andrault, D., Fiquet, G., Guyot, F., Hanfland, M., 1998. Pressure-induced Landau-type transition in stishovite, Science 282, 720-724.

Anselment, B., 1985. The dynamics of the phase transition of rutile in the $CaCl_2$ type for the example of $CaBr_2$ and for the polymorphism of $CaCl_2$, Thesis, University of Karlsruhe.

Bärnighausen, H., Bossert, W., Anselment, B., 1984. A second-order phase transition of calcium bromide and its geometrical interpretation, Acta Crystallogr. A 40, C96.

348 Bolfan-Casanova, N., Andrault, D., Amiguet, E., Guignot, N., 2009. Equation of state and
349 post-stishovite transforamtion of Al-bearing silica up to 100 Gpa and 3000 K, Phys. Earth
350 Planet. Inter. 174, 70-77.
351 Brodholt, J.P., Helffrich, G., Trampert, J., 2007. Chemical versus thermal heterogeneity in the
352 lower mantle: The most likely role of anelasticity, Earth Planet. Sci. Lett., 262, 429-437.
353 Carpenter, M.A., 2006. Elastic properties of minerals and the influence of phase transitions,
354 Am. Mineral. 91, 229-246.
355 Carpenter, M.A., Buckley, A., Taylor, P.A., Darling, T.W., 2010. Elastic relaxations associate
356 with the $Pm\bar{3}m$-$R\bar{3}c$ transition in $LaAlO_3$: III. Superattenuation of acoustic resonances, J.
357 Phys.: Condens. Matter 22, 035405.
358 Carpenter, M.A., Hemley, R.J., Mao, H., 2000. High-pressure elasticity of stishovite and the
359 $P4_2/mnm \leftrightarrow Pnnm$ phase transition, J. Geophys. Res. 105, 10807-10816.
360 Carpenter, M.A., Salje, E.K.H., Braeme-Barber, A., Wruck, B., Dove, M.T., Knight, K.S.,
361 1998. Calibration of excess thermodynamic properties and elastic constant variations
362 associated with the $\alpha \leftrightarrow \beta$ phase transition in quartz, Am. Mineral. 83, 2-22.
363 Carpenter, M.A., Zhang, Z., 2011. Anelasticity maps for acoustic dissipation associated with
364 phase transitions in minerals, Geophys. J. Int. 186, 279-295.
365 Cohen, R.E., 1992. High pressure research: application to earth and planetary science.
366 American Geophysical Union, Washington, D.C., 425.
367 Cohen, R.E., 1994. First-principles theory of crystalline SiO_2. In Heaney, P.J., Prewitt, C.T.,
368 and Gibbs, G.V., Eds., Silica: Physical Behavior, Geochemistry, and Materials Applications,
369 29, 369-402. Reviews in Mineralogy, Mineralogical Society of America, Chantilly, Virginia.
370 Combs, J.A., Yip, S., 1983. Single-kink dynamics in a one-dimentional atomic chain: a
371 nonlinear atomistic theory and numerical simulation, Phys. Rev. B 28, 6873-6885.
372 Cordier, P., Mainprice, D., Mosenfelder, J.L., 2004. Mechanical instability near the stishovite-

$CaCl_2$ phase transition: Implication for crystal preferred orientations and seismic properties, Eur. J. Mineral. 16, 387-399.

Daraktchiev, M., Harrison, R.J., Mountstevens, E.H., Redfern, S.A.T., 2006. Effect of transformation twins on the anelastic behavior of polycrystalline $Ca_{1-x}Sr_xTiO_3$ and $Sr_xBa_{1-x}SnO_3$ perovskite in relation to the seismic properties of Earth's mantle perovskite, Mater. Sci. Eng. A 442, 199-203.

Daraktchiev, M., Salje, E.K.H., Lee, W.T., Redfern, S.A.T., 2007. Effect of internal friction on transformation twin dynamics in perovskite $Sr_xBa_{1-x}SnO_3$ (x=0.6, 0.8), Phys. Rev. B 75, 134102.

Driver, K.P., Cohen, R.E., Wu, Z., Militzer, B., Rios, P.L., Towler, M.D., Needs, R.J., Wilkins, J.W., 2010. Quantum Monte Carlo computations of phase stability, equations of state, and elasticity of high-pressure silica. Proc. Natl. Acad. Sci. USA 107, 9519.

Dubrovinsky, L.S., Belonoshko, A.B, 1996. Pressure-induced phase transition and structural changes under deviatoric stress of stishovite to $CaCl_2$-like structure. Geochim. Cosmochim. Acta 60, 3657-3663.

Faul, U.H., Jackson I., 2005. The seismological signature of temperature and grain size variations in the upper mantle, Earth Planet. Sci. Lett. 234, 119-134.

Fritz, I.J., 1974. Pressure and temperature dependences of the elastic properties of rutile (TiO_2), J. Phys. Chem. 35, 817-826.

Gung, Y., Romanowicz, B., 2004. Q tomography of the upper mantle using three-component long-period waveforms, Geophys. J. Int. 157, 813-830.

Hahn, C., Unruh, H.G., 1991. Comment on tempeature-induced structural phase transition in $CaBr_2$ studied by Raman spectroscopy, Phys. Rev. B 43, 12665-12667.

Haines, J., Leger, J.M., 1993. Phase transitions in ruthenium dioxide up to 40 GPa: Mechanism for the rutile-to-fluorite phase transformation and a model for the high-pressure

behaviour of stishovite SiO_2, Phys. Rev. B 48, 13344-13350.

Haines, J., Leger, J.M., 1997. X-ray diffraction study of the phase transitions and structural evoluation of tin oxides at high pressure: Relationships between structure types and implications for other rutile-type dioxides, Phys. Rev. B 55, 11144-11154.

Haines, J., Leger, J.M., Chateau C., Bini, R., Ulivi, L., 1998. Ferroelastic phase transition in rutile-type germanium dioxide at high pressure, Phys. Rev. B 58, R2909-R2919.

Haines, J., Leger, J.M., Chateau, C., Pereira, A.S., 2000. Structural evolution of rutile-type and $CaCl_2$-type germanium dioxide at high pressure, Phys. Chem. Miner. 27, 575-582.

Haines, J., Leger, J.M., Gorelli, F., Klug, D.D., Tse, J.S., Li, Z.Q., 2001. X-ray diffraction and theoretical studies of the high-pressure structure and phase transition in magnesium fluoride, Phys. Rev. B 64, 134110.

Haines, J., Leger, J.M., Howau, S., 1995. Second-order rutile-type to $CaCl_2$-type phase transition in β-MnO_2 at high pressure, J. Phys. Chem. Solids, 56, 965-973.

Haines, J., Leger, J.M., Schulte, O., 1996. The high-pressure phase transition sequence from rutile-type through to the contunnite-type structure in PbO_2, J. Phys.: Condens. Matter 8, 1631-1646.

Haines, J., Leger, J.M., Schulte, O., Hull, S., 1997. Neutron diffraction study of the ambient-pressure, rutile-type and the high-pressure, $CaCl_2$-type phases of ruthenium dioxide. Acta Crystallogr. B 53, 880-884.

Harrison, R.J., Redfern, S.A.T., 2002. The influence of transformation twins on the seismic-frequency elastic and anelastic properties of perovskite: Dynamical mechanical analysis of single crystal $LaAlO_3$, Phys. Earth Planet. Inter. 134, 253-272.

Harrison, R.J., Redfern, S.A.T., Bismayer, U., 2004a. Seismic-frequency attenuation at first-order phase transitions: Dynamical mechanical analysis of pure and Ca-doped lead orthophosphate, Mineral. Mag. 68, 839-852.

Harrison, R.J., Redfern, S.A.T., Buckley, A., Salje, E.K.H., 2004b. Application of real-time, stroboscopic x-ray diffraction with dynamical mechanical analysis to characterize the motion of ferroelastic domain walls, J. Appl. Phys. 95, 1706-1717.

Harrison, R.J., Redfern, S.A.T., Salje, E.K.H., 2004c. Dynamical excitation and anelastic relaxation of ferroelastic domain walls in $LaAlO_3$, Phys. Rev. B 69, 144101.

Harrision, R.J., Redfern, S.A.T., Street, J., 2003. The effect of transformation twins on the seismic-frequency mechanical properties of polycrystalline $Ca_{1-x}Sr_xTiO_3$ perovskite, Am. Mineral. 88, 574-582.

Hellwig, H., Goncharov, A.F., Gregoryanz, E., Mao, H.K., Hemley, R.J., 2003. Brillouin and Raman spectroscopy of the ferroelastic rutile-to-$CaCl_2$ transition in SnO_2 at high pressure, Phys. Rev. B 67, 174110.

Hemley, R.J., Mao, H.K., Gramsch, S.A., 2000a. Pressure-induced transformations in deep mantle and core minerals, Mineral. Mag. 64, 157-184.

Hemley, R.J., Prewitt, C.T., Kingma, K.J., 1994. High-pressure behaviour of silica. In Heaney, P.J., Prewitt, C.T., and Gibbs, G.V., Eds., Silica: Physical Behavior, Geochemistry, and Materials Applications, 29, 41-81. Reviews in Mineralogy, Mineralogical Society of America, Chantilly, Virginia.

Hemley, R.J., Shu, J., Carpenter, M.A., Hu, J., Mao, H.K., Kingma, K.J., 2000b. Strain/order parameter coupling in the ferroelastic transition in dense SiO_2, Solid State Commun. 114, 527-532.

Howard, C.J., Kennedy, B.J., Curfs, C., 2005. Temperature-induced structural changes in $CaCl_2$, $CaBr_2$, and $CrCl_2$: A synchrotron x-ray powder diffraction study, Phys. Rev. B 72, 214114.

Huang, Y.N., Wang, Y.N., Shen, H.M., 1992. Internal friction and dielectric loss related to domain walls, Phys. Rev. B 46, 3290-3295.

448 Jackson, I., 2007. Physical origins of anelasticity and attenuation in rocks, in Mineral Physics,
449 Treatise on Geophysics (ed. Price, G.D., Oxford, Elsevier), 2, 493-525.
450 Jackson, I., Fitz Gerald, J.D., Faul, U.H., Tan, B.H., 2002. Grain-size-sensitive seismic wave
451 attenuation in polycrystalline olivine, J. Geophys. Res. 107, 2360.
452 Jiang, F., Gwanmesia, G.D., Dyuzheva, T.I., Duffy, T.S., 2009. Elasticity of stishovite and
453 acoustic mode softening under high pressure by Brillouin scattering, Phys. Earth Planet. Inter.
454 172, 235-240.
455 Kanchana, V., Vaitheeswaran, G., Rajagopalan, M., 2003. High-pressure structural phase
456 transitions in magnesium fluoride studied by electronic structure calculations, J. Alloys
457 Compd. 352, 60-65.
458 Kaneshima, S., Helffrich, G., 2010. Small scale heterogeneity in the mid-lower mantle
459 beneath the circum-Pacific area, Phys. Earth Planet. Inter. 183, 91-103.
460 Karato, S.I., Karki, B.B., 2001. Origin of lateral variation of seismic wave velocities and
461 density in the deep mantle, J. Geophys. Res. 106, 21771-21783.
462 Karki, B.B., Stixrude, L, and Crain, J., 1997a. Ab initio elasticity of three high-pressure
463 polymorphs of silica, Geophys. Res. Lett. 24, 3269-3272.
464 Karki, B.B., Warren, M.C., Stixrude, L, Ackland, G.J., Crain, J., 1997b. Ab initio studies of
465 high-pressure structural transformations in silica, Phys. Rev. B 55, 3465-3471.
466 Kennedy, B.J., Howard, C.J., 2004. Synchrotron x-ray powder diffraction study of the
467 structural phase transition in $CaBr_2$, Phys. Rev. B 70, 144102.
468 Kingma, K.J., Cohen, R.E., Hemley, R.J., Mao, H.K., 1995. Transformation of stishovite to a
469 denser phase at lower-mantle pressures, Nature 374, 243-245.
470 Kingma, K.J., Mao, H.K., Hemley, R.J., 1996. Synchrotron x-ray diffraction of SiO_2 to
471 multimegabar pressures, High Pressure Res. 14, 363-374.
472 Kusaba, K., Kilegawa, T., 2008a. In situ X-ray observation of phase transitions in ZnF_2 under

high pressure and high temperature, Solid State Commun. 145, 279-282.

Kusaba, K., Kikegawa, T., 2008b. Stable phase with the α-PbO_2 type structure in MgF_2 under high pressure and high temperature, Solid State Commun. 148, 440-443.

Lacks, D.J., Gordon, R.G., 1993. Calculations of pressure-induced phase transitions in silica, J. Geophys. Res. 98, 22147-22155.

Lakes, R.S., 2004. Viscoelastic measurement techniques, Rev. Sci. Instrum. 75, 797-810.

Lakshtanov, D.L., Litasov, K.D., Sinogeikin, S.V., Hellwig, H., Ohtani, E., Bass, J.D., 2007a. Effect of Al^{3+} and H^{+} on the elastic properties of stishovite, Am. Mineral. 92, 1026-1030.

Lakshtanov, D., Sinogeikin, S.V., Litasov, K.D., Prakapenka, V.B., Hellwig, H., Wang, J., Sanches-Valle, C., Perrillat, J.P., Chen, B., Somayazulu, M., Li, J., Ohtani, E., Bass, D., 2007b, The post-stishovite phase transition in hydrous alumina-bearing SiO_2 in the lower mantle of the earth, Proc. Natl. Acad. Sci. USA 104, 13588-13590.

Lee, C., Gonze, X., 1995. The pressure-induced ferroelastic phase transition of SiO_2 stishovite, J. Phys.: Condens. Matter 7, 3693-3698.

Lee, C., Gonze, X., 1997. SiO_2 stishovite under high pressure: dielectric and dynamical properties and the ferroelastic phase transition, Phys. Rev. B 56, 7321-7330.

Lee, T., Lakes, R.S., Lal. A., 2000. Resonant ultrasound spectroscopy for measurement of mechanical damping: comparison with broadband viscoelastic spectroscopy, Rev. Sci. Instrum. 71, 2855-2861.

Lekic, V., Matas, J., Panning, M., Romanowicz, B., 2009. Measurement and implications of frequency dependence of attenuation, Earth Planet. Sci. Lett. 282, 285-293.

Lodziana, Z., Parlinski, K., Hafner, J., 2001. Ab initio studies of high-pressure transformations in GeO_2, Phys. Rev. B 63, 134106.

Mao, H.K., Shu, J., Hu, J., Hemley, R.J., 1994. Single-crystal X-ray diffraction of stishovite to 65 GPa, EOS Transactions of the American Geophysical Union, 75, 662.

Matas, J., Bukowinski, M.S.T., 2007. On the anelastic contribution to the temperature dependence of lower mantle seismic velocities, Earth Planet. Sci. Lett. 259, 51-65.

Matsui, Y., Tsuneyuki, S., 1992. Molecular dynamics study of rutile-$CaCl_2$-type phase transitions of SiO_2, in High Pressure Research: Application to Earth and Planetary Sciences, (eds. Syono, Y. and Manghani, M.H., Terra Scientific Publishing Company, American Geophysical Union, Washington, D.C.) 67, 433-439.

McKnight, R.E.A., Carpenter, M.A., Darling, T.W., Buckley, A., Taylor, P.A., 2007. Acoustic dissipation associated with phase transitions in lawsonite, $CaAl_2Si_2O_7(OH)_2{\cdot}H_2O$, Am. Mineral. 92, 1665-1672.

McKnight, R.E.A., Howard, C.J., Carpenter, M.A., 2009a. Elastic anomalies associated with transformation sequencies in perovskites: I. Strontium zirconate, $SrZrO_3$, J. Phys.: Condens. Matter 21, 015901.

McKnight, R.E.A., Howard, C.J., Carpenter, M.A., 2009b. Elastic anomalies associated with transformation sequencies in perovskites: II. The strontium zirconate-titanate $Sr(Zr,Ti)O_3$ solid solution series, J. Phys.: Condens. Matter 21, 015902.

McKnight, R.E.A., Moxon, T., Buckley, A., Taylor, P.A., Darling, T.W., Carpenter, M.A., 2008. Grain size dependence of elastic anomalies accompanying the α-β phase transition in polycrystalline quartz, J. Phys.: Condens. Matter 20, 075229.

Mechie, J., Sobolev, S.V., Ratschbacher, L., Babeyko, A.Y., Bock, G., Jones, A.G., Nelson, K.D., Solon, K.D., Brown, L.D., Zhao, W., 2004. Precise temperature estimation in the Tibetan crust from seismic detection of the α-β quartz transition, Geology 32, 601-604.

Migliori, A., Maynard, J.D., 2005. Implementation of a modern resonant ultrasound spectroscopy system for the measurement of the elastic moduli of small solid specimens, Rev. Sci. Instrum. 76, 121301.

Nagel, L., OKeeffe, M., 1971. Pressure and stress induced polymorphism of compounds with

523 rutile structure, Mater. Res. Bull. 6, 1317-1320.
524 Nomura, R., Hirose, K., Sata, N., Ohishi, Y., 2010. Precise determination of post-stishovite
525 phase transition boundary and implications for seismic heterogeneities in the mid-lower
526 mantle, Phys. Earth Planet. Inter. 183, 104-109.
527 Nowick, A.S., Berry, B.S., 1972. Anelastic Relaxation in Crystalline Solids (New York:
528 Academic).
529 Ono, S., Hirose, K., Murakami, M., Isshiki, M., 2002a. Post-stishovite phase boundary in
530 SiO_2 determined by in situe X-ray observations, Earth Planet. Sci. Lett. 197, 187-192.
531 Ono, S., Hirose, K., Murakami, M., Isshiki, M., 2002b. Phase boundary between rutile-type
532 and $CaCl_2$-type germanium dioxide determined by in situ X-ray observations, Am. Mineral.
533 87, 99-102.
534 Ono, S, Mibe, K., 2011. Determination of the phase boundary of the ferroelastic rutile to
535 $CaCl_2$ transition in RuO_2 using in situ high-pressure and high-temperature Raman
536 spectroscopy, Phys. Rev. B 84, 054114.
537 Parlinski, K., Kawazoe, Y., 2000. Ab initio study of phonons in the rutile structure of SnO_2
538 under pressure, Eur. Phys. J. B 13, 679-683.
539 Patnaik, P., 2002. Handbook of Inorganic Chemicals, McGraw-Hill.
540 Perakis, A., Lampakis, D., Boulmetis, Y.C., Raptis, C., 2005. High-pressure Raman study of
541 the ferroelastic rutile-o-$CaCl_2$ phase transition in ZnF_2, Phys. Rev. B 72, 144108.
542 Raptis, C., McGreevy, R.L., 1991. Reply to “Comment on ‘Temperature-induced structural
543 phase transition in $CaBr_2$ studied by Raman spectroscopy’”, Phys. Rev. B 43, 12668-12669.
544 Raptis, C., McGreevy, R.L., Seguier, D.G., 1989. Temperature-induced structural phase
545 transition in $CaBr_2$ studied by Raman spectroscopy, Phys. Rev. B 39, 7996-7999.
546 Ren, F., Case, E.D., Morrison, A., Tafesse, M., Baumann, M.J., 2009. Resonant ultrasound
547 spectroscopy measurement of Young’s modulus, shear modulus and Poisson’s ratio as a

548 function of porosity for alumina and hydroxygapatite, Philosophical Magazine 89, 1163-1182.
549 Romanowicz, B., 1995. A global tomographic model of shear attenuation in the upper mantle.
550 J. Geophys. Res. 100, 12375-12394.
551 Salje, E.K.H., 2008. (An)elastic softening from static grain boundaries and possible effects on
552 seismic wave propagation, Phys. Chem. Miner. 35, 321-330.
553 Shieh, S.R., Duffy, T.S., Li, B., 2002. Strength and elasticity of SiO_2 across the stishovite-
554 $CaCl_2$-type structural phase boundary, Phys. Rev. Lett. 89, 255507.
555 Shieh, S.R., Duffy, T.S., Shen, G., 2005. X-ray diffraction study of phase stability in SiO_2 at
556 deep mantle conditions, Earth Planet. Sci. Lett. 235, 273-282.
557 Tan, B.H., Jackson, I., Fitz Gerald, J.D., 2001. High-temperature viscoelasticity of fine-
558 grained polycrystalline olivine, Phys. Chem. Miner. 28, 641-664.
559 Togo, A., Oba, F., Tanaka, I., 2008. First-principles calculations of the ferroelastic transition
560 between rutile-type and $CaCl_2$-type SiO_2 at high pressures, Phys. Rev. B 78, 134106.
561 Tsuchida, Y., Yagi, T., 1989. A new, post-stishovite high-pressure polymorph of silica, Nature
562 340, 217-220.
563 Tsuchiya, T., Caracas, R., Tsuchiya, J., 2004. First principles determination of the phase
564 boundary of high-pressure polymorphs of silica, Geophys. Res. Lett. 31, L11610.
565 Unruh, H.G., 1993. Ferroelastic phase transitions in calcium chloride and calcium bromide,
566 Phase Transit. 45, 77.
567 Unruh, H.G., 1995. Soft modes at ferroelastic phase transitions, Phase Transit. 55, 155-168.
568 Unruh, H.G., Mhlenberg, D., Hahn, Ch., 1992. Ferroelastic phase transition in $CaCl_2$ studied
569 by Raman spectroscopy, Z. Phys. B Condens. Matter 86, 133-138.
570 Valgoma, J.A., Perez-Mato, J.M., Garcia, A., Schwarz, K., Blaha, P., 2002. First-principles
571 study of the ferroelastic phase transition in $CaCl_2$, Phys. Rev. B 65, 134104.
572 Vinnik, L.P., Oreshin, S.I., Speziale, S., Weber, M., 2010. Mid-mantle layering from SKS

receiver functions, Geophys. Res. Lett. 37, L24302.

Walsh, J.N., Taylor, P.A., Buckley, A., Darling, T.W., Schreuer, J., Carpenter, M.A., 2008. Elastic and anelastic anomalies in (Ca,Sr)TiO_3 perovskites: analogue behaviour for silicate perovskites, Phys. Earth Planet. Inter. 167, 110-117.

Wang, H., Liu, X., Li, Y., Liu, Y., Ma, Y., 2011. First-principles study of phase transitions in antiferromagnetic XF_2 (X=Fe, Co and Ni), Solid State Commun. 151, 1475-1478.

Wang, Y.N., Huang, Y.N., Shen, H.M., Zhang, Z.F., 1996. Mechanical and dielectric energy loss related to viscous motion and freezing of domain walls. J. Phys. IV France 6, C8-505-C8-514.

Webb, S., Jackson, I., 2003. Anelasticity and microcreep in polycrystalline MgO at high temperature: an exploratory study, Phys. Chem. Miner. 30, 157-166.

Zhang, L., Wang, Y., Cui, T., Li, Y., Li, Y., He, Z., Ma, Y., Zou, G., 2007. $CaCl_2$-type high-pressure phase of magnesium hydride predicted by ab initio phonon calculations, Phys. Rev. B 75, 144109.

Zhang, L., Wang, Y., Cui, Ma, Y., Zou, G., 2008. First-principles study of the pressure-induced rutile-$CaCl_2$ phase transition in MgF_2, Solid State Commun. 145, 283-287.

Zhang, Z., Koppensteiner, J., Schranz, W., Betts, J.B., Migliori, A., and Carpenter, M.A., 2010a. Microstructure dynamics in orthorhombic perovskites, Phys. Rev. B 82, 014113.

Zhang, Z., Koppensteiner, J., Schranz, W., Carpenter, M.A., 2010b. Anelastic loss behaviour of mobile microstructures in $SrZr_{1-x}Ti_xO_3$ perovskites, J. Phys.: Condens. Matter 22, 295401.

FIGURE CAPTIONS

Fig. 1. Stacks of RUS scans for $CaCl_2$. (a) High temperatures. Regularly spaced background peaks are due to the alumina buffer rods. (b) Low temperatures. The background peaks at very low temperatures are noise from somewhere in the sample holder.

Fig. 2. (Color online) Temperature dependences of shear modulus G and inverse quality factor Q^{-1} of $CaCl_2$ determined by RUS. The dashed line is the transition temperature 491 K (given by Bärnighausen et al. 1984; Anselment 1985; Unruh et al. 1992; Unruh 1993). The dash-dotted curve shows the pattern of loss behaviour.

Fig. 3. (Color online) Temperature dependences of storage modulus E' and dissipation $\tan\delta$ measured at different frequencies (0.1 – 50 Hz) by DMA for $CaCl_2$ during cooling with the cooling rate of 3 K/min. The temperature dependences of shear modulus G and inverse of quality factor Q^{-1} determined by RUS at high frequencies ~0.3 MHz are also shown for comparison. The dashed line is the transition temperature 491 K (given by Bärnighausen et al. 1984; Anselment 1985; Unruh et al. 1992; Unruh 1993). Increases in $\tan\delta$ at high temperatures are most likely due to the influence of grain boundaries.

Fig. 4. Schematic form of elastic constant variations expected for a pseudoproper ferroelastic tetragonal $\leftrightarrow$ orthorhombic phase transition (from Fig. 9 of Carpenter and Salje 1998).

Table 1

Summary of transition temperature for $CaCl_2$ detected using different methods.

Method	Sample	Transition temperature (K)	Reference
XRD	powder	491	Bärnighausen et al. 1984
XRD	powder	491	Anselment 1985
Raman Spectroscopy	pellet	491	Unruh et al. 1992; Unruh 1993
Synchrotron XRD	powder	508	Howard et al. 2005

637 **Figures**

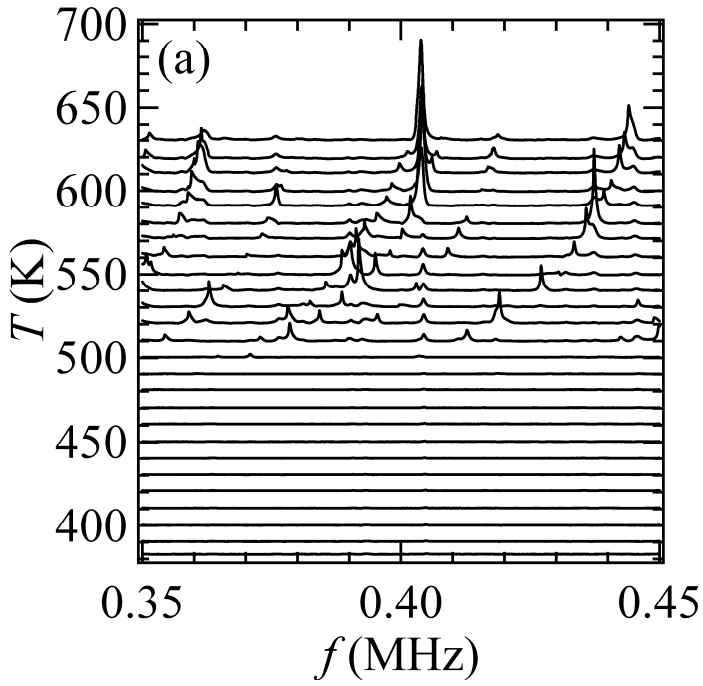

638

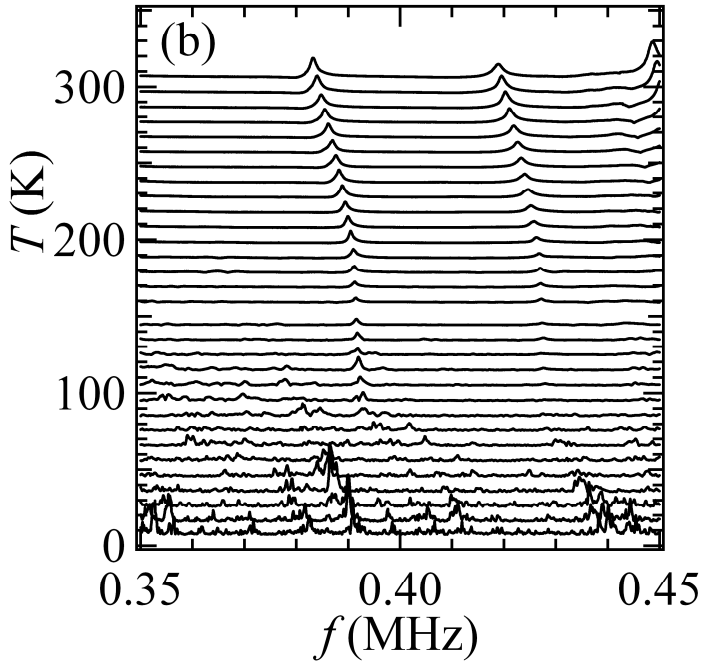

639

640 **Fig. 1.** Stacks of RUS scans for $CaCl_2$. (a) High temperatures. Regularly spaced background
641 peaks are due to the alumina buffer rods. (b) Low temperatures. The background peaks at very
642 low temperatures are noise from somewhere in the sample holder.

643

644

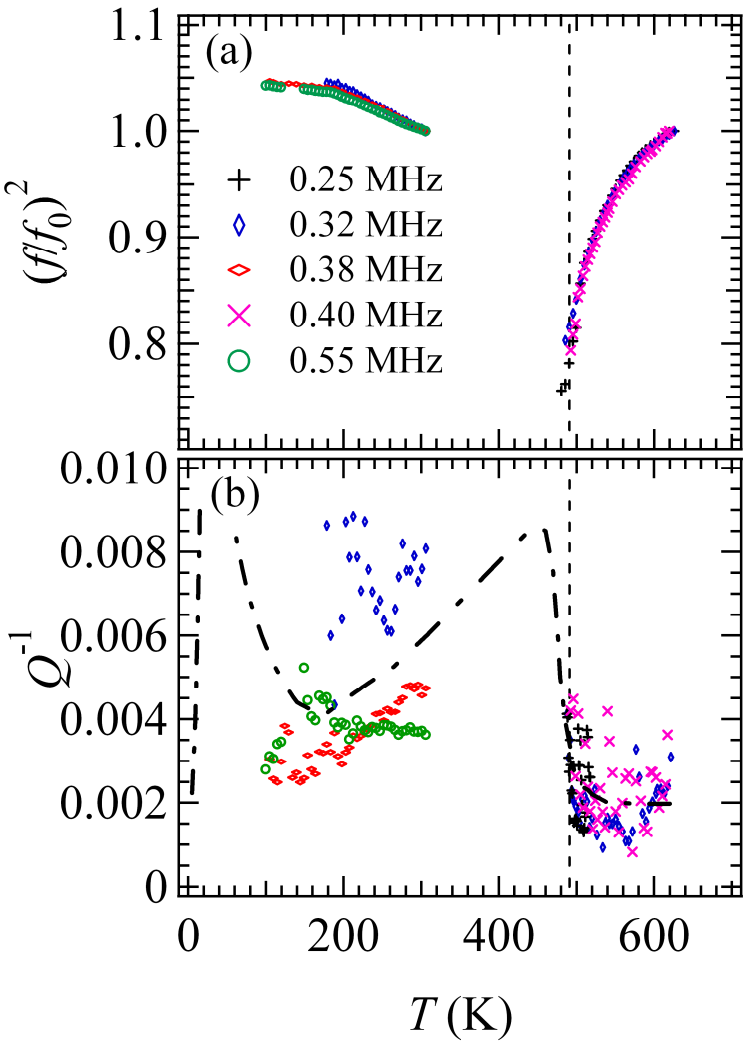

Fig. 2. (Color online) Temperature dependences of shear modulus G and inverse quality factor Q^{-1} of $CaCl_2$ determined by RUS. The dashed line is the transition temperature 491 K (given by Bärnighausen et al. 1984; Anselment 1985; Unruh et al. 1992; Unruh 1993). The dash-dotted curve shows the pattern of loss behaviour.

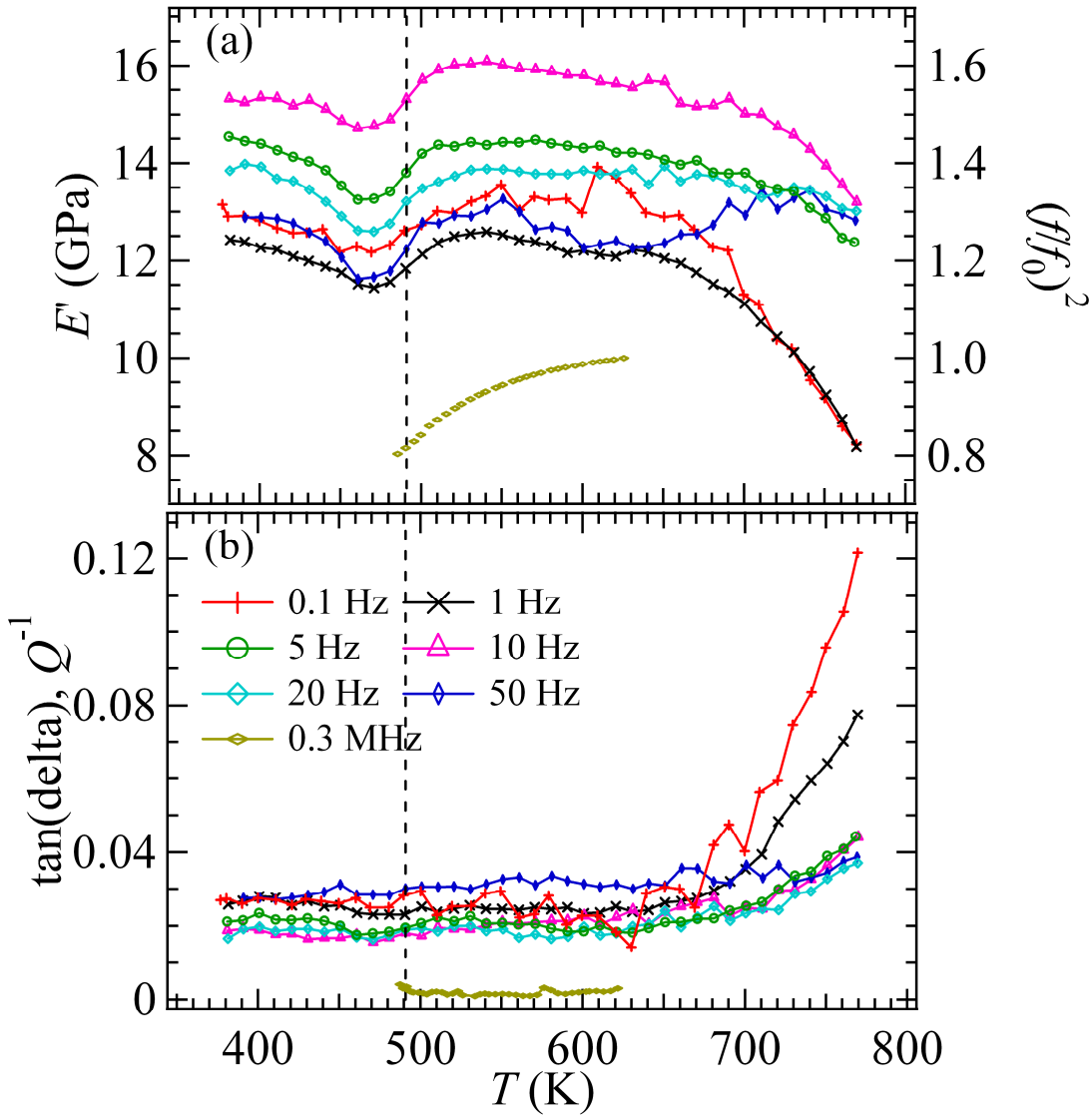

Fig. 3. (Color online) Temperature dependences of storage modulus *E*' and dissipation tanD measured at different frequencies (0.1 – 50 Hz) by DMA for $CaCl_2$ during cooling with the cooling rate of 3 K/min. The temperature dependences of shear modulus *G* and inverse of quality factor Q^{-1} determined by RUS at high frequencies ~0.3 MHz are also shown for comparison. The dashed line is the transition temperature 491 K (given by Bärnighausen et al. 1984; Anselment 1985; Unruh et al. 1992; Unruh 1993). Increases in tanδ at high temperatures are most likely due to the influence of grain boundaries.

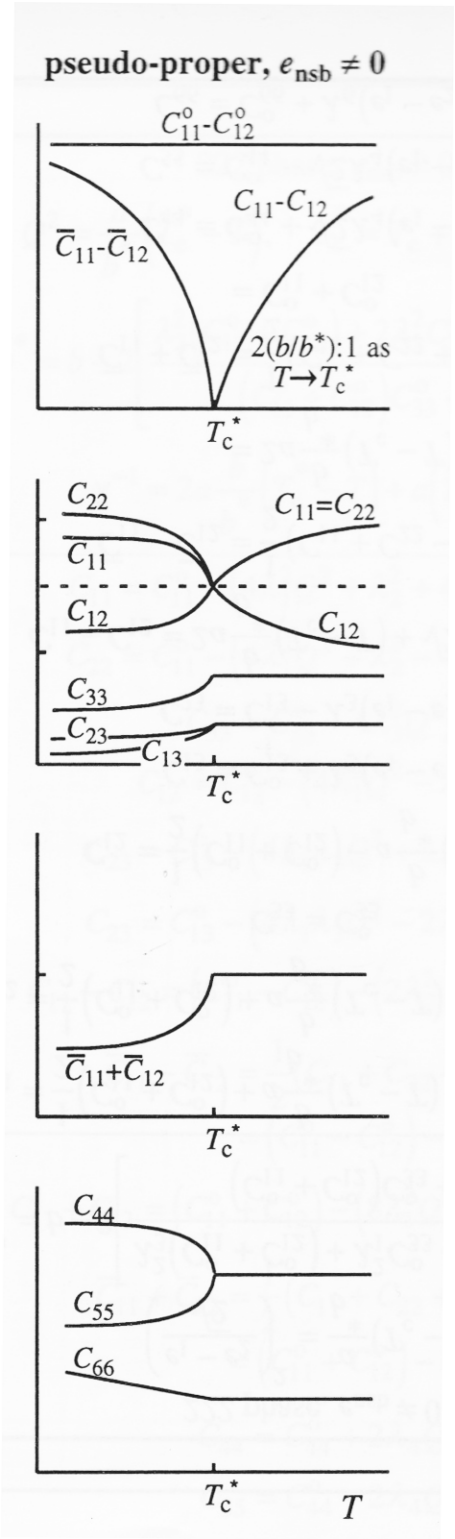

Fig. 4. Schematic form of elastic constant variations expected for a pseudoproper ferroelastic tetragonal ↔ orthorhombic phase transition (from Fig. 9 of Carpenter and Salje 1998).